Sliding Mode Speed Control of Induction Motor Using SVPWM Technique for Hybrid Electric Vehicles

Priyanka Malla
M. Tech Scholor, Department of Electrical Engineering, AMET University, Chennai, Tamilnadu India E-mail: priyamallaece@gmail.com

***Abstract*—In this paper, sliding mode control (SMC) with space vector modulation (SVM) is presented for speed control of induction motor (IM) drive. The IM is an attractive option for variable speed drive applications which are required for electric vehicles. The speed and flux responses are enhanced in SMC with SVM. IM control using SMC with SVM and SVM based Proportional Integral (PI) control are compared. SMC with SVM method is developed to design a system which has the desired dynamic behavior and is robust with respect to perturbations. Lyapunov stability analysis is used for stable performance of the system. MATLAB/Simulink platform is used for simulations to validate the proposed system.**

Keywords— Sliding mode control, inverter, induction motor, Space vector modulation.

I. INTRODUCTION

Hybrid Electric Vehicles (HEVs) use an internal combustion engine (ICE) and an electric motor, hence the name Hybrid. HEV can solve the problems of decreasing fossil fuel and atmospheric pollution. Electric vehicles are becoming popular recently due to having facilities of eco-friendly and simple controlling nature [1-3]. According to the requirements of an HEV induction motor is a suitable choice for its drive motor [1, 3]. Induction motor is a nonlinear system, multivariable and strong coupling hence the speed control is not easy [4-5]. With the advent of semiconductor devices and microprocessors induction motor found its use in changeable speed applications [6-7]. Induction motor has the advantages of low cost, efficiency being high and less maintenance [6]. PI control of induction motor had the disadvantage of high overshoot, sluggish response and fixed gain constants [6]. Vector control and direct torque control (DTC) are the main methods of control of induction motors [6-10].

Article details:

Received: March 2021, Revision: Aug. 2021, Accepted: Nov. 2021, Publication: January 2022.

Citation of paper: Priyanka Malla, "Sliding Mode Speed Control of Induction Motor Using SVPWM Technique for Hybrid Electric Vehicles", *International Journal of New Technologies in Science and Engineering (IJNTSE)*, Vol. 8,, Issue. 1, pp. no, January, 2022.

*Corresponding author:

In vector control torque and flux can be controlled independently by decoupling the two components of stator current under transient and steady state conditions [11-12]. Compared to vector control DTC enhances the static and transient responses and also it is less sensitive to uncertainties and parameter variation [6, 13]. B. Chikondra et. al, presented many strategies for DTC of five phase induction motor drive and enhanced the performance under fault [14-18]. However, the disadvantage of DTC was temperature rise of the motor and noise production. Direct Self Control (DSC) was presented by Depenbrock [19] and Direct Torque Control was presented by Takahashi and Noguchi [20]. The inverter failure is reported by authors in [21] for induction motor driven electric vehicle. High performance finite control and neural network based predictive controllers are developed for induction motor drives by authors in [22-24]. Among the available methods sliding mode control is most suitable for induction motor drives because it is a nonlinear control method [25]. SMC is a control method in which the control structure is changed when the state of the system changes to get a desired response [26]. SMC has the advantage of insensitivity to parameter variations and disturbances. The disadvantage of SMC was the chattering phenomenon [25].

Many scholars are proposed different motor-drives for application of electric vehicles. The authors in [27-28] presented the sensorless predictive controller of PMBLDC motor drive for electric vehicle application. The battery playing significant role in electric vehicles, authors in [29-32] reported different strategies for battery power sharing in electric vehicles. Moreover, the inverter plays a major role in electric vehicle in order to provide supply to induction motor. The authors are proposed reduced switches of inverter in [33] for application of electric vehicle. Further the authors [34-35] reported the significance benefits of multilevel inverter for induction motor drive. Authors in [36] developed matrix converter based induction motor drive. The switching losses of inverter fed induction motor with SVPWM are examined by authors in [37]. In this paper induction motor control using SMC with SVM has been presented. Induction motor control using PI control is also examined. A comparison is made between the two control methods. Induction motor control using SMC with SVM results in less speed ripple. SVM results in robustness to disturbances and reduction in amount of harmonics in the output voltage. The organization of this paper is as stated. The d-q model of induction motor in stationary reference frame is given in section-II. The SVM technique is discussed in section-III. Section-IV gives the design of SM controller. Section-V gives the result of simulation for SMC and conclusion is followed by Section-VI.

II. Dynamic Model Of Induction Motor

The modeling based on d-q frame of induction motor is attempted by using references [6-7] with the help of below equations.

$$\begin{bmatrix} u_\beta \\ u_\alpha \\ v_0 \end{bmatrix} = \frac{2}{3}\begin{bmatrix} 1 & \frac{-1}{2} & \frac{-1}{2} \\ 0 & \frac{-\sqrt{3}}{2} & \frac{\sqrt{3}}{2} \\ 0.5 & 0.5 & 0.5 \end{bmatrix}\begin{bmatrix} v_{as} \\ v_{bs} \\ v_{cs} \end{bmatrix} \tag{1}$$

$$u_\beta = \frac{2}{3}v_{an} - \frac{1}{3}v_{bn} - \frac{1}{3}v_{cn} \tag{2}$$

$$u_\alpha = -\frac{1}{\sqrt{3}}v_{bn} + \frac{1}{\sqrt{3}}v_{cn} \tag{3}$$

$$u_\alpha = R_s i_\alpha + \frac{d}{dt}\psi_{\alpha s} \tag{4}$$

$$u_\beta = R_s i_\beta + \frac{d}{dt}\psi_{\beta s} \tag{5}$$

However, the rotor has been short-circuited, hence the voltage at rotor terminals are zero and those can be represented as

$$0 = R_r i_{\beta r} + \frac{d}{dt}\psi_{\beta r} - \omega_r \psi_{\alpha r} \tag{6}$$

$$0 = R_r i_{\alpha r} + \frac{d}{dt}\psi_{\alpha r} - \omega_r \psi_{\beta r} \tag{7}$$

$$\psi_{\alpha s} = L_s i_{\alpha s} + L_m i_{\alpha r} \tag{8}$$

$$\psi_{\alpha r} = L_r i_{\alpha r} + L_m i_{\alpha s} \tag{9}$$

$$\psi_{\beta s} = L_s i_{\beta s} + L_m i_{\beta r} \tag{10}$$

$$\psi_{\beta r} = L_r i_{\beta r} + L_m i_{\beta s} \tag{11}$$

$$\frac{d\psi_\alpha}{dt} = -\frac{R_r}{L_r}\psi_\alpha - \omega\psi_\beta + R_r\frac{L_m}{L_r}i_\alpha \tag{12}$$

$$\frac{d\psi_\beta}{dt} = -\frac{R_r}{L_r}\psi_\beta + \omega\psi_\alpha + R_r\frac{L_m}{L_r}i_\beta \tag{13}$$

$$\frac{di_\alpha}{dt} = \frac{L_r}{L_s L_r - L_m^2}\left(-\frac{L_m}{L_r}\frac{d\psi_\alpha}{dt} - R_s i_\alpha + u_\alpha\right) \tag{14}$$

$$\frac{di_\beta}{dt} = \frac{L_r}{L_s L_r - L_m^2}\left(-\frac{L_m}{L_r}\frac{d\psi_\beta}{dt} - R_s i_\beta + u_\beta\right) \tag{15}$$

$$\frac{d\omega}{dt} = \frac{p}{J}(T - T_L) \tag{16}$$

Therefore the torque generated by motor is expressed by eq (17)

$$T = \frac{3p}{2}\frac{L_m}{L_r}(i_\beta\psi_\alpha - i_\alpha\psi_\beta) \tag{17}$$

$$\psi = [\psi_\alpha \psi_\beta]^T \tag{18}$$

$$i = [i_\alpha i_\beta]^T \tag{19}$$

$$u = [u_\alpha u_\beta]^T \tag{20}$$

III. Space Vector PWM

SVPWM method is the best PWM technique. SVPWM method results in fewer harmonic in the output voltage. SVPWM uses the principle of a rotating space vector. A space vector V with magnitude V_m rotating in a circular path at angular velocity ω is produced when induction motor is powered. There are 8 switching states in a three phase inverter. The detailed SVPWM representation is depicted in Fig. 1.

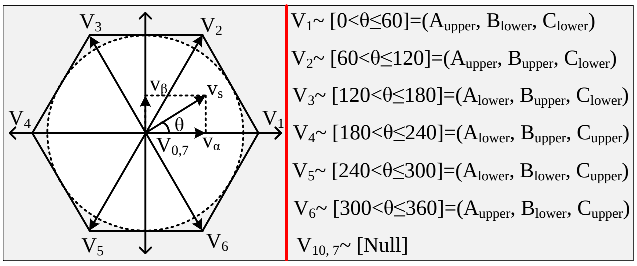

Fig. 1: Representation of SVPWM technique

For the implementation of space vector PWM, transformation has been made of the voltage equations from the abc to the stationary αβ reference frame (i.e., eq(1))

Relationship between these two reference frames is

$$\left|v_{ref}\right| = \sqrt{u_\alpha^2 + u_\beta^2}\ ,\ \alpha = \tan^{-1}\frac{u_\beta}{u_\alpha} = \omega t = 2\pi f t \tag{21}$$

$$\int_0^{T_Z}\overline{V_{ref}}\,dt = \int_0^{T_1}\overline{V_1}\,dt + \int_{T_1}^{T_1+T_2}\overline{V_2}\,dt + \int_{T_Z-T_1}^{T_Z}\overline{V_0}\,dt \tag{22}$$

$$T_z\overline{V}_{ref} = T_1\overline{V_1} + T_2\overline{V_2} \tag{23}$$

$$T_z\left|v_{ref}\right|\begin{bmatrix}\cos\alpha \\ \sin\alpha\end{bmatrix} = T_1\frac{2}{3}V_{dc}\begin{bmatrix}1 \\ 0\end{bmatrix} + T_1\frac{2}{3}V_{dc}\begin{bmatrix}\cos(\frac{\pi}{3}) \\ \sin(\frac{\pi}{3})\end{bmatrix} \tag{24}$$

$$\text{where } 0 \le \alpha \le 60$$

$$T_1 = T_Z\ \ a\frac{\sin(\frac{\pi}{3} - \alpha)}{\sin(\frac{\pi}{3})} \tag{25}$$

$$T_2 = T_Z\ \ a\frac{\sin(\alpha)}{\sin(\frac{\pi}{3})} \tag{26}$$

$$T_0 = T_z - (T_1 + T_2)\ \text{where}\ T_Z = \frac{1}{f}\ \text{and}\ a = \left|\frac{\overline{v_{ref}}}{\frac{2}{3}v_{dc}}\right| \tag{27}$$

$$T_1 = \frac{\sqrt{3}T_z\left|v_{ref}\right|}{v_{dc}}\left(\sin\left(\frac{\pi}{3} - \alpha + \frac{n-1}{3}\pi\right)\right) \tag{28}$$

$$=\frac{\sqrt{3}T_z\left|v_{ref}\right|}{V_{dc}}\left(\sin\left(\frac{n\pi}{3}-\alpha\right)\right) \quad (29)$$

$$T_2=\frac{\sqrt{3}T_z\left|v_{ref}\right|}{V_{dc}}\left(\sin\left(\alpha-\frac{n-1}{3}\pi\right)\right) \quad (30)$$

$$T_0=T_z-(T_1+T_2) \quad (31)$$

The required pulses of inverter to drive the induction motor can be obtained by using above time periods. The detailed block diagram of sliding mode controller based speed control of induction motor is shown in Fig. 2. The PI controller based speed control of induction motor is shown in Fig. 3.

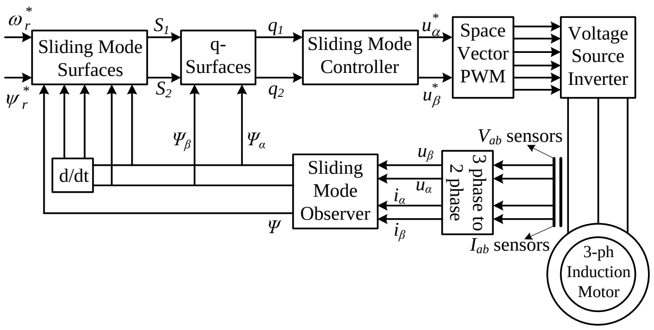

Fig. 2: Block diagram of sliding mode control with SVM technique

IV. Sliding Mode Controller Design

The response of the control system depends on choice of the sliding surfaces. For the inverter fed induction motor SMC is implemented by defining two sliding surfaces.

$$S_1=C_1(\omega_r-\omega_r)+\frac{d}{dt}(\omega_r-\omega_r) \quad (32)$$

$$S_1=C_2(\psi_r-\psi_r)+\frac{d}{dt}(\psi_r-\psi_r) \quad (33)$$

The positive constant C_1 and C_2 determine the convergent speed of rotor speed ω_r and rotor flux ψ_r, where ω_r and ψ_r are the desired speed and desired rotor flux respectively, ω_r and ψ_r are the actual rotor speed and actual rotor flux, and $\psi_r=\sqrt{\psi_\alpha^2+\psi_\beta^2}$, where ψ_α and ψ_β are the actual rotor fluxes in (α,β) reference frame. The behavior of the system is governed by $S_1=0$ and $S_2=0$ when SMC occurs. The system is forced to track these sliding surfaces. Now the actual speed and actual rotor flux will follow the desired rotor speed and desired rotor flux respectively.

Invariant transformation of sliding surfaces:

The design process can be simplified. By decoupling S w.r.t. two phase stator voltage vectors $u=\left[u_\alpha u_\beta\right]^T$, the system motion can be projected in subspaces S_1 and S_2

$$\frac{ds}{dt}=F+Au \quad (34)$$

Where $F=\ [f_1 f_2]^T$, $u=\ [u_\alpha u_\beta]^T$ and $S=[S_1 S_2]^T$

By differentiating the surfaces S_1 and S_2 and using equations from the dynamic model of induction motor functions f_1, f_2 and matrix A can be found. f_1, f_2 do not depend on u_α or u_β and the matrix A is given by

$$A=\begin{bmatrix} a_1\hat{\psi}_\beta & a_1\hat{\psi}_\alpha \\ a_2\hat{\psi}_\alpha & a_2\hat{\psi}_\beta \end{bmatrix} \quad (35)$$

Where $\sigma={1}/{(L_sL_r-L_m^2)}$

$$\gamma=L_rR_s+L_sR_r$$

$$a_1=\left(\frac{3P}{2J}\right)\sigma\, L_m$$

$$a_2=-\left(\frac{1}{\hat{\psi}_r}\right)\sigma\, R_rL_m$$

As f_1, f_2 do not depend on u_α or u_β, using the transformed sliding surfaces $q=\ [q_1q_2]^T$ the design can be simplified and Lyapunov stability analysis can be used. q surfaces and S surfaces are related by an invariant transformation

$$q=A^TS \quad (36)$$

This transformation provides an easy implementation of SMC technique. The discontinuity surface transformation from $S=0$ to $q=0$ does not affect the control.

Lyapunov method of stability analysis:

Lyapunov function $v=\frac{1}{2}S^TS\geq 0$

$$v=S^T(F+Au) \quad (37)$$

The control law is selected as

$$u_\alpha=-b_1\,\mathrm{sgn}(q_1)-b_2q_1 \quad (38)$$

$$u_\beta=-b_1\,\mathrm{sgn}(q_2)-b_2q_2 \quad (39)$$

Where

$$\mathrm{sgn}(q)=\begin{cases}+1, q>0\\-1, q<0\end{cases}$$

b_1, b_2 are constants.

Stability of the SMC: If $v=S^TS<0$ the reaching condition of SMC is satisfied, then the control system will become stable. For this b_1, b_2 are chosen so that $(b_1+b_2|q_m|)>\max(\ f_m^*)$,. , $m=1,2$.

Then $$v=S^TS=S^T(F+Au)=\left(q_1f_1^*-b_1|q_1|-b_2q_1^2\right)+\left(q_2f_2^*-b_1|q_2|-b_2q_2^2\right) \quad (40)$$

Where $\left[f_1^*f_2^*\right]=(A^{-1}F)^T$

It is found from above equation that if $\left(b_1 + b_2|q_m|\right) > \max\left(f_m^*\right), \quad m = 1,2$ is chosen then $v < 0$. Therefore the origin in space q and in S also is asymptotically stable and stable sliding mode exists. The speed ω_r and the flux ψ_r will track their command signals respectively.

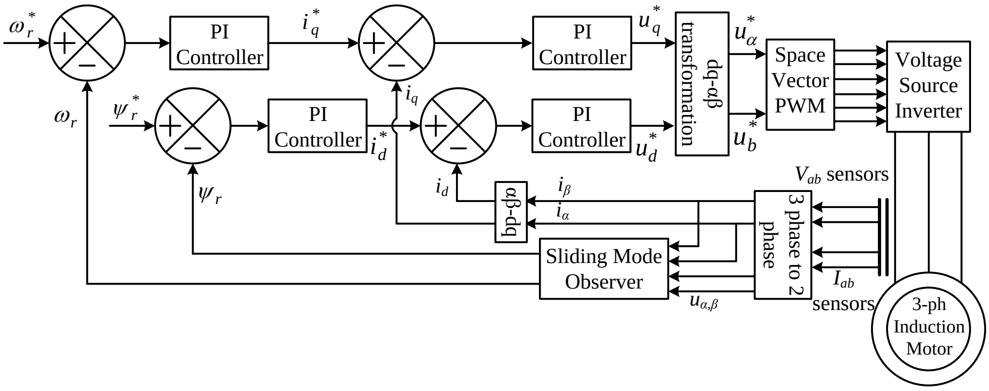

Fig. 3: Block diagram of speed control with PI controller

The sliding mode technique generates chattering and causes ripple in speed, flux and current in the system. Here sliding mode technique with SVM produces less harmonic distortion and reduces the chattering.

V. Simulation and Results

Results of SMC with SVM are carried out by using MATLAB/Simulink. These results are compared with the simulation result of PI control of induction motor. SMC with SVM do not require any speed sensor. Block diagram of induction motor speed control with SMC and PI control are shown in Figure 2 and 3 respectively. In the SMC with SVM method u_α^* and u_β^* are derived from the control law (38) and (39)

$$\sqrt{u_\alpha^{*2} + u_\beta^{*2}} = |u_s| \quad \text{and} \quad \theta = \tan^{-1}\frac{|u_\beta|}{|u_\alpha|}$$

The PI control parameters are tuned by trial and error method. In the proposed scheme the gating pulses for the inverter are got by using SMC with SVM method. The induction motor parameters are listed in below table:

S. No	Parameter	Value
1	Rated voltage (v)	24
2	Rated Speed (rad/s)	24
3	Rated flux (m Wb)	10
4	Pole pairs	1
5	Inertia constant (Nms^2)	0.000433
6	Stator inductance (mH)	0.59
7	Rotor inductance (mH)	0.59
8	Mutual inductance (mH)	0.555
9	Stator resistance (ohm)	0.0106
10	Rotor resistance (ohm)	0.0118

The inverter switching frequency is chosen as 10.5 kHz. The parameters b_1 and b_2 are chosen as $b_1 = 0.1$ and $b_2 = 0.3$ for SMC with SVM.

The simulation results are obtained for flux and speed response for different speeds. The results of SMC with SVM are compared with the PI control method. The harmonic distortion is high in case of PI controller than for SMC with SVM method. The rotor flux tracks the reference flux with greater accuracy in case of SMC with SVM than in case of PI controller which has oscillations and overshoots. In the SMC with SVM method the oscillations in speed are less.

Speed tracking

The speed response was observed with various types of signals. The speed was observed for positive speed and then speed reversal. The speed response was checked for low speeds also. The speed response was checked for 21.82 % of rated speed (50 rpm), 43.64 % of rated speed (100 rpm) and rated speed of 230 rpm. The response for sinusoidal speed tracking was also observed. For rated speed induction motor is subjected to changes in speed at different instants of time according to the following cycle:
Time = [0 0.1 2.9 3 3.1 6 6.1],
Speed = [0 230 230 0 -230 -230 0]

For 21.82 % of rated speed (50 rpm) and 43.64 % of rated speed (100 rpm) a square wave speed reference cycle was used. The total time for the cycle was 6 seconds and the speed reversed after 3 seconds for both the cases.

The response of torque with SMC is depicted in Fig. 4 for changing load torque from 1 N.m to -1 N.m. The corresponding steady state response of currents is presented in Fig. 5. The speed response of induction motor with SMC and PI are shown in Fig. 6 and Fig. 7 respectively. Corresponding speed error in SMC and PI controller are reported in Fig. 8 and Fig. 9 respectively. Responses of flux are depicted in Fig. 10 and Fig. 11 respectively of induction motor with SMC and PI controller.

Responses of induction motor speed is depicted for 21.82% and 43.64% change in rated speed from Fig. 12 to Fig. 15 with SMC and PI controller. From these figures, clearly it is showing that SMC responses are superior to PI and having significant priority to use SMC for eclectic vehicle application.

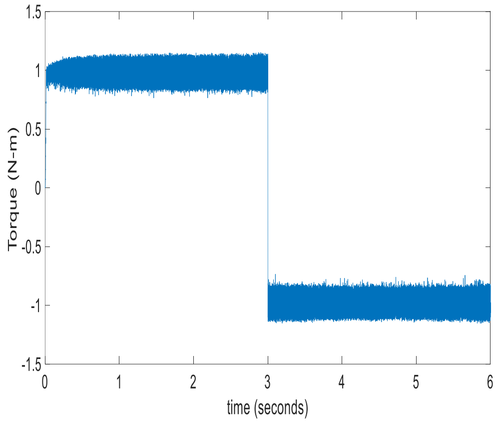

Fig. 4: Torque response for rated speed for SMC

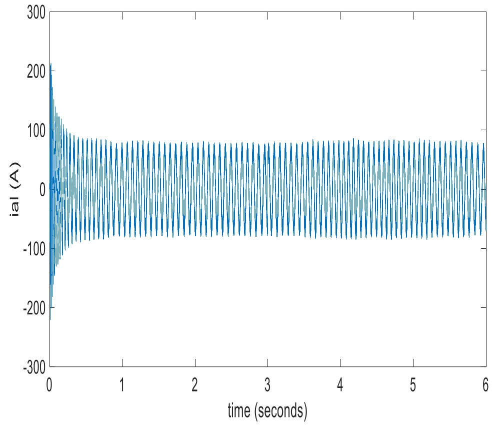

Fig. 5: Stator current at rated speed for SMC

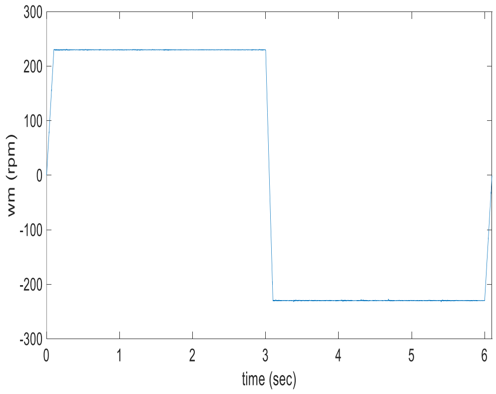

Fig. 6: Speed response for rated speed for SMC with speed reversal

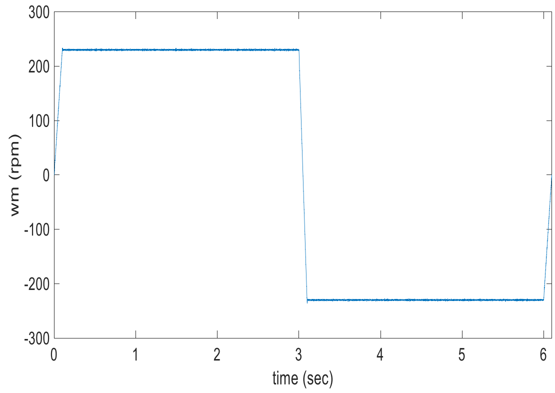

Fig. 7: Speed response for rated speed for PI control with speed reversal

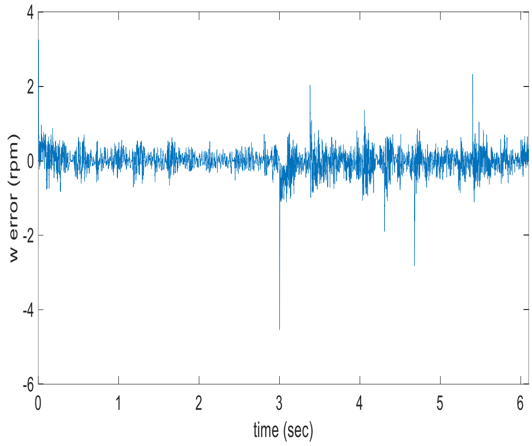

Fig. 8: Speed error at rated speed for SMC

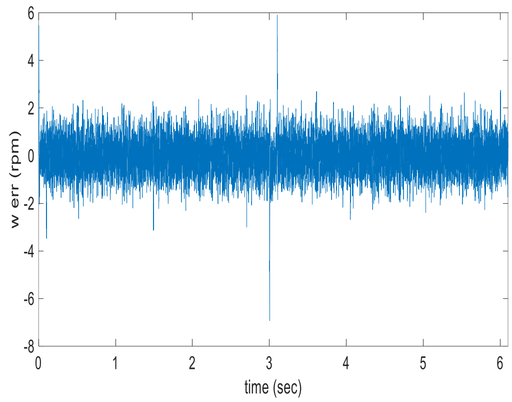

Fig. 9: Speed error at rated speed for PI control.

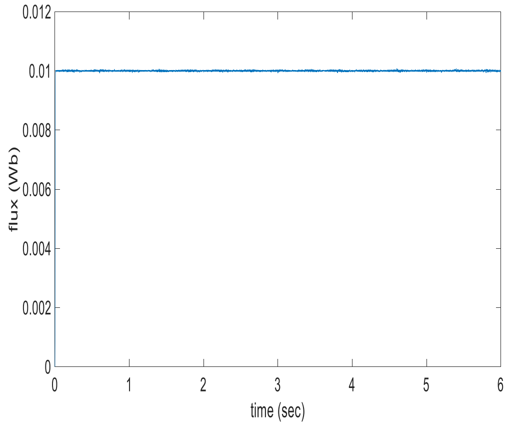

Fig. 10: Flux response for SMC

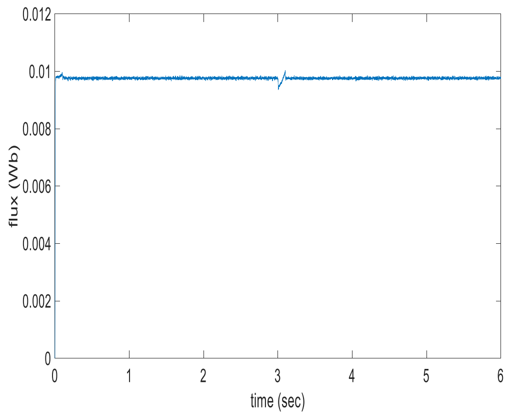

Fig. 11: Flux response for PI control

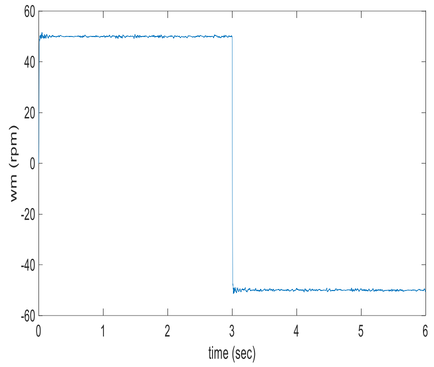

Fig. 12: Speed response with SMC for about 21.82% of rated speed with speed reversal

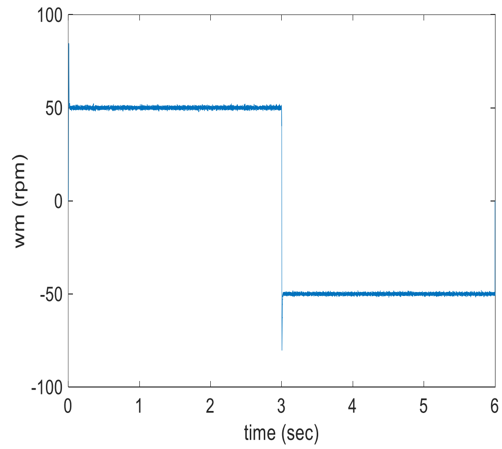

Fig. 13: Speed response with PI control for about 21.82% of rated speed with speed reversal

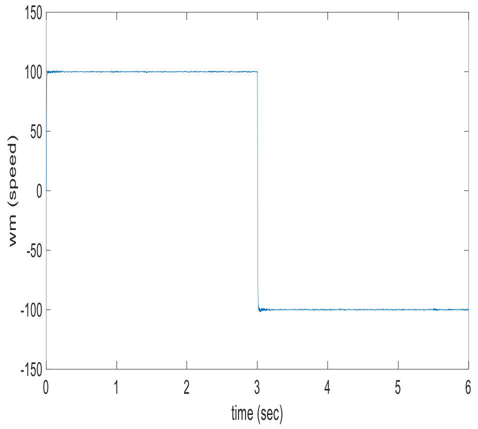

Fig. 14: Speed response for SMC for about 43.64%of rated speed with speed reversal

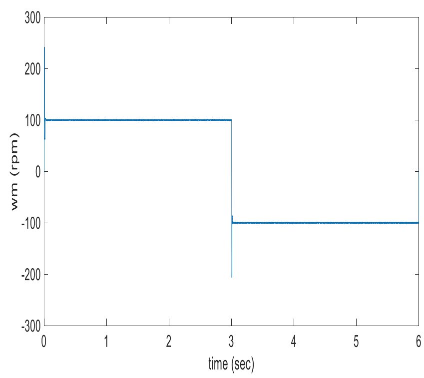

Fig. 15: Speed response for PI control for about 43.64%of rated speed with speed reversal

VI. Conclusion

A speed control approach using SMC combined with SVPWM is presented in this paper. The actual speed and flux signals track the reference speed and flux signals with good accuracy. The speed control of induction motor for low speeds is difficult. For low speeds also the response was accurate with SMC with SVPWM method. The simulation is done for different types of speed signal tracking. The obtained results for sliding mode control technique with SVPWM are compared with the classical PI control method. The PI control method has more overshoot; rise time and speed ripple as compared with the SMC with SVPWM method. Sliding mode with SVM presents good control characteristics and the response is independent of load disturbances.

References

[1]. U. R. Muduli, et. al, “An Improved Direct Torque Control with Battery Power Management of Open-End Winding Induction Motor Drive for Electric Vehicles,” *2020 IEEE Energy Conversion Congress and Exposition (ECCE)*, 2020, pp. 6332-6337, doi: 10.1109/ECCE44975.2020.9236199.

[2]. Dr. Siva Ganesh Malla, Priyanka Malla and Rajesh Koilada, “Solar Energy based Hybrid Electric Car: Part 1”, International Journal of New Technologies in Science and Engineering (IJNTSE), Vol. 6, Issue 6, pp. 11- 25, Dec. 2019.

[3]. U. R. Muduli and R. K. Behera, “A Modified High Gain Boost TNPC Inverter with Neutral Point Balancing for Three-Phase Induction Motor Driven Electric Vehicle,” *2020 IEEE International Conference on Power Electronics, Drives and Energy Systems (PEDES)*, 2020, pp. 1-6, doi: 10.1109/PEDES49360.2020.9379556.

[4]. U. Ranjan M and R. K. Behera, “Constant Switching Frequency DTC SVPWM with Reduced Common Mode Voltage for Two Level Five Phase Induction Motor Drives,” *2018 IEEE International Conference on Power Electronics, Drives and Energy Systems (PEDES)*, 2018, pp. 1-6, doi: 10.1109/PEDES.2018.8707765.

[5]. B. Chikondra, Utkal. R. M and R. Kumar Behera, “Fault-Tolerant DTC Technique for Five-phase Three-Level NPC Inverter-fed Induction Motor Drive with an Open-Phase Fault,” *2019 IEEE Energy Conversion Congress and Exposition (ECCE)*, 2019, pp. 5281-5287, doi: 10.1109/ECCE.2019.8912513.

[6]. S. G. Malla, "A review on Direct Torque Control (DTC) of induction motor: With applications of fuzzy," *2016 International Conference on Electrical, Electronics, and Optimization Techniques (ICEEOT)*, 2016, pp. 4557-4567, doi: 10.1109/ICEEOT.2016.7755579.

[7]. B. K. Bose, “Modern Power Electronics and AC Drives, 2001

[8]. U. R. Muduli and R. K. Behera, “Virtual Vector based SVPWM-DTC for Five-Phase Two-Level VSI fed Induction Motor Drive,” *2021 1st International Conference on Power Electronics and Energy (ICPEE)*, 2021, pp. 1-6, doi: 10.1109/ICPEE50452.2021.9358755.

[9]. U. R. Muduli, B. Chikondra and R. K. Behera, “Space Vector PWM Based DTC Scheme With Reduced Common Mode Voltage for Five-Phase Induction Motor Drive,” *IEEE Transactions on Power Electronics*, vol. 37, no. 1, pp. 114-124, Jan. 2022, doi: 10.1109/TPEL.2021.3092259.

[10]. B. Chikondra, U. R. Muduli and R. K. Behera, “An Improved DTC Technique for Three-Level NPC VSI Fed Five-Phase Induction Motor Drive to Eliminate Common Mode Voltage,” *2019 National Power Electronics Conference (NPEC)*, 2019, pp. 1-6, doi: 10.1109/NPEC47332.2019.9034720.

[11]. S. G. Malla, C. N. Bhende and S. Mishra, “Photovoltaic based water pumping system,” *2011 International Conference on Energy, Automation and Signal*, 2011, pp. 1-4, doi: 10.1109/ICEAS.2011.6147148.

[12]. Bhende, Chandrashekhar N. and Malla, Siva G. “Novel Control of Photovoltaic based Water Pumping System without Energy Storage”, *International Journal of Emerging Electric Power Systems*, vol. 13, no. 5, 2012. https://doi.org/10.1515/1553-779X.2931

[13]. J. M. R. Malla and S. G. Malla, "Three level diode clamped inverter for DTC-SVM of induction motor," *2010 Joint International Conference on Power Electronics, Drives and Energy Systems & 2010 Power India*, 2010, pp. 1-6, doi: 10.1109/PEDES.2010.5712447.

[14]. B. Chikondra, U. R. Muduli and R. K. Behera, “Fault-Tolerant DTC Technique for an Inverter-Fed Five-Phase Induction Motor Drive with an Open-Phase Fault,” *2019 21st European Conference on Power Electronics and Applications (EPE '19 ECCE Europe)*, 2019, pp. P.1-P.10, doi: 10.23919/EPE.2019.8914993.

[15]. B. Chikondra, U. R. Muduli and R. K. Behera, “An Improved Open-Phase Fault-Tolerant DTC Technique for Five-Phase Induction Motor Drive Based on Virtual Vectors Assessment,” *IEEE Transactions on Industrial Electronics*, vol. 68, no. 6, pp. 4598-4609, June 2021, doi: 10.1109/TIE.2020.2992018.

[16]. B. Chikondra, U. R. Muduli and R. K. Behera, “Open-Phase Fault-Tolerant Direct Torque Control for Five-Phase Three-Level NPC VSI fed Induction Motor Drive,” *2020 IEEE International Conference on Power Electronics, Drives and Energy Systems (PEDES)*, 2020, pp. 1-6, doi: 10.1109/PEDES49360.2020.9379786.

[17]. U. R. Muduli, B. Chikondra and R. K. Behera, “Virtual Vector based DTC with CMV Reduction for Five-Phase Induction Motor Drive,” *2020 3rd International Conference on Energy, Power and Environment: Towards Clean Energy Technologies*, 2021, pp. 1-6, doi: 10.1109/ICEPE50861.2021.9404393.

[18]. B. Chikondra, U. R. Muduli and R. K. Behera, “Improved DTC Technique for THL-NPC VSI Fed Five-Phase Induction Motor Drive Based on VVs Assessment Over a Wide Speed Range,” *IEEE Transactions on Power Electronics*, vol. 37, no. 2, pp. 1972-1981, Feb. 2022, doi: 10.1109/TPEL.2021.3102963.

[19]. Depenbrock M. Direct self-control (DSC) of inverter fed induktion machine. In1987 IEEE Power Electronics Specialists Conference 1987 Jun 21 (pp. 632-641). IEEE. https://doi.org/10.1109/pesc.1987.7077236

[20]. Jain S, Sharma S, Mandloi RS. Improved Power Quality AC Drive Feeding Induction Motor. IJETEE. 2013 Apr;2(1):35-40.

[21]. U. R. Muduli, et. al., “Interrupt-Free Operation of Dual-Motor Four-Wheel Drive Electric Vehicle Under Inverter Failure,” *IEEE Transactions on Transportation Electrification*, vol. 7, no. 1, pp. 329-338, March 2021, doi: 10.1109/TTE.2020.2997354.

[22]. U. R. Muduli and R. Kumar Behera, “High Performance Finite Control Set Model Predictive DTC for Three-to-Five Phase Direct Matrix Converter Fed Induction Motor Drive,” *2021 22nd IEEE International Conference on Industrial Technology (ICIT)*, 2021, pp. 198-202, doi: 10.1109/ICIT46573.2021.9453475.

[23]. U. R. Muduli, K. Al Jaafari and R. K. Behera, “Optimized Neural Network Based Predictive Maintenance for Five-Phase Induction Motor Failure,” *2021 IEEE 12th Energy Conversion Congress & Exposition - Asia (ECCE-Asia)*, 2021, pp. 1537-1541, doi: 10.1109/ECCE-Asia49820.2021.9478989.

[24]. U. R. Muduli, B. Chikondra and R. K. Behera, “Novel Model Predictive DTC for Three-to-Five Phase Direct Matrix Converter Fed Induction Motor Drive,” *2021 IEEE 12th Energy Conversion Congress & Exposition - Asia (ECCE-Asia)*, 2021, pp. 1505-1510, doi: 10.1109/ECCE-Asia49820.2021.9479067.

[25]. Aichi B, Bourahla M, Kendouci K, “Real-time hybrid control of induction motor using sliding mode and pi anti-windup”, *2018 International Conference on Electrical Sciences and Technologies in Maghreb (CISTEM)*, 2018 Oct 28 (pp. 1-6). IEEE. https://doi.org/10.1109/cistem.2018.8613320.

[26]. Young KD, Utkin VI, Ozguner U, “A control engineer's guide to sliding mode control”, *IEEE transactions on control systems technology,*. 1999 May; Vol. 7(3): pp. 328-42. https://doi.org/10.1109/87.761053.

[27]. P. Kumar, et. al., “Iron-Loss Modeling With Sensorless Predictive Control of PMBLDC Motor Drive for Electric Vehicle Application,” *IEEE Transactions on Transportation Electrification*, vol. 7, no. 3, pp. 1506-1515, Sept. 2021, doi: 10.1109/TTE.2020.3036991.

[28]. P. Kumar, et. al., “An Enhanced Linear Active Disturbance Rejection Controller for High Performance PMBLDCM Drive Considering Iron Loss,” *IEEE Transactions on Power Electronics*, vol. 36, no. 12, pp. 14087-14097, Dec. 2021, doi: 10.1109/TPEL.2021.3088418.

[29]. U. R. Muduli, et. al., “Predictive Control based Battery Power Sharing for Four-Wheel Drive Electric Vehicle,” *2021 IEEE Applied Power Electronics Conference and Exposition (APEC)*, 2021, pp. 817-821, doi: 10.1109/APEC42165.2021.9487084.

[30]. U. R. Muduli, et. al., “Predictive Control with Battery Power Sharing Scheme for Dual Open-End Winding Induction Motor based Four-Wheel Drive Electric Vehicle,” *IEEE Transactions on Industrial Electronics*, doi: 10.1109/TIE.2021.3091919.

[31]. U. R. Muduli, et. al, “Predictive Battery SoC Control for Dual Propulsion Differential Four Wheel Drive Electric Vehicle,” *2021 IEEE Energy Conversion Congress and Exposition (ECCE)*, 2021, pp. 1490-1495, doi: 10.1109/ECCE47101.2021.9595587.

[32]. U. R. Muduli, et. al, “Cell Balancing of Li-ion Battery Pack with Adaptive Generalised Extended State Observers for Electric Vehicle Applications,” *2021 IEEE Energy Conversion Congress and Exposition (ECCE)*, 2021, pp. 143-147, doi: 10.1109/ECCE47101.2021.9595601.

[33]. S. K. Baksi, et al., “Reduced Switch Count Three-Phase Five-Level Boosted ANPC Inverter with Unipolar PWM Scheme for Electric Vehicle Propulsion Drive,” *IECON 2021 – 47th Annual Conference of the IEEE Industrial Electronics Society*, 2021, pp. 1-6, doi: 10.1109/IECON48115.2021.9589916.

[34]. B. Ch, U. R. Muduli and R. K. Behera, “Performance Comparison of Five-Phase Three-Level NPC to Five-Phase Two-Level Voltage Source Inverter,” *2018 IEEE International Conference on Power Electronics, Drives and Energy Systems (PEDES)*, 2018, pp. 1-6, doi: 10.1109/PEDES.2018.8707510.

[35]. B. Chikondra, U. R. Muduli and R. K. Behera, “Performance Comparison of Five-Phase Three-Level NPC to Five-Phase Two-Level VSI,” *IEEE Transactions on Industry Applications*, vol. 56, no. 4, pp. 3767-3775, July-Aug. 2020, doi: 10.1109/TIA.2020.2988014.

[36]. U. R. Muduli, B. Chikondra and R. K. Behera, “Direct Torque Control of 3x5 Matrix Converter Fed Five-Phase IM Drive using Virtual Vector Concept,” *2021 IEEE Applied Power Electronics Conference and Exposition (APEC)*, 2021, pp. 765-770, doi: 10.1109/APEC42165.2021.9487140.

[37]. U. R. Muduli, B. Chikondra and R. K. Behera, “Continuous and Discontinuous SVPWM with Switching Loss Control for Five-Phase Two-Level VSI fed Induction Motor Drive,” *2020 IEEE International Conference on Power Electronics, Drives and Energy Systems (PEDES)*, 2020, pp. 1-6, doi: 10.1109/PEDES49360.2020.9379717.